Incorporating a Hybrid Urease–Carbon Nanotubes Sensitive Nanofilm on Capacitive Field-Effect Sensors for Urea Detection

ARTICLE *in* ANALYTICAL CHEMISTRY · MAY 2014

Impact Factor: 5.64 · DOI: 10.1021/ac500458s · Source: PubMed

4 AUTHORS, INCLUDING:

José Roberto Siqueira Jr.
Universidade Federal do Triangulo Mineiro (U…

25 PUBLICATIONS **530** CITATIONS

analytical chemistry

Article

pubs.acs.org/ac

Incorporating a Hybrid Urease-Carbon Nanotubes Sensitive Nanofilm on Capacitive Field-Effect Sensors for Urea Detection

José R. Siqueira, Jr.,*[,†] Denise Molinnus,[‡] Stefan Beging,[‡] and Michael J. Schöning*[,‡,§]

[†]Institute of Exact Sciences, Naturals and Education, Federal University of Triângulo Mineiro (UFTM), 38064-200 Uberaba, Brazil

[‡]Institute of Nano- and Biotechnologies (INB), FH Aachen, Campus Jülich, 52428 Jülich, Germany

[§]Peter Grünberg Institute (PGI-8), Forschungszentrum Jülich, 52425 Jülich, Germany

Supporting Information

ABSTRACT: The ideal combination among biomolecules and nanomaterials is the key for reaching biosensing units with high sensitivity. The challenge, however, is to find out a stable and sensitive film architecture that can be incorporated on the sensor's surface. In this paper, we report on the benefits of incorporating a layer-by-layer (LbL) nanofilm of polyamidoamine (PAMAM) dendrimer and carbon nanotubes (CNTs) on capacitive electrolyte-insulator-semiconductor (EIS) field-effect sensors for detecting urea. Three sensor arrangements were studied in order to investigate the adequate film architecture, involving the LbL film with the enzyme urease: (i) urease immobilized directly onto a bare EIS [EIS-urease] sensor; (ii) urease atop the LbL film over the EIS [EIS-(PAMAM/CNT)-urease] sensor; and (iii) urease sandwiched between the LbL film and another CNT layer [EIS-(PAMAM/CNT)-urease-CNT]. The surface morphology of all three urea-based EIS biosensors was investigated by atomic force microscopy (AFM), while the biosensing abilities were studied by means of capacitance−voltage (*C*/*V*) and dynamic constant-capacitance (ConCap) measureaments at urea concentrations ranging from 0.1 mM to 100 mM. The EIS-urease and EIS-(PAMAM/CNT)-urease sensors showed similar sensitivity (∼18 mV/decade) and a nonregular signal behavior as the urea concentration increased. On the other hand, the EIS-(PAMAM/CNT)-urease-CNT sensor exhibited a superior output signal performance and higher sensitivity of about 33 mV/decade. The presence of the additional CNT layer was decisive to achieve a urea based EIS sensor with enhanced properties. Such sensitive architecture demonstrates that the incorporation of an adequate hybrid enzyme-nanofilm as sensing unit opens new prospects for biosensing applications using the field-effect sensor platform.

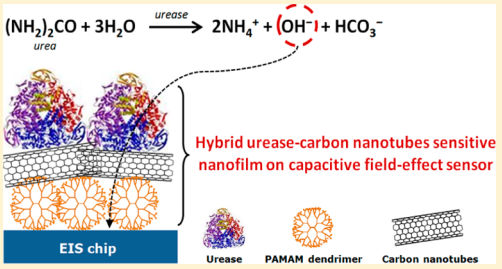

The manipulation of bio- and nanomaterials has permitted the development of new sensitive hybrid nanostructures for biosensing applications. Depending on the biosystem under study, specific techniques and strategies should be carefully selected for the formation of such nanostructures as well as the adequate choice of the transduction mode responsible for the sensor's response signal.[1−6] In particular, field-effect devices (FEDs), a special class of silicon-based sensors that are advantageous for sensing and biosensing, are suitable for biomedical applications, exhibiting advantages in terms of miniaturized processing and reliable biological recognition at small concentrations.[7−9] The capacitive electrolyte-insulator-semiconductor (EIS) structure is a typical class of sensors based on FEDs. Basically, the introduction of an additional ion- and/or charge-sensitive gate layer leads to changes in the electrical surface charge of the EIS surface, modulating its capacitance.[7−9]

The key to achieve a specific biosensor with preserved activity, high sensitivity, and selectivity rises from the employed method to immobilize an enzyme on the EIS chip. Particularly, the adequate combination of biomolecules and nanomaterials, such as enzymes and carbon nanotubes, respectively, can be manipulated in nanostructured layer-by-layer (LbL) films, in which materials are disposed in a controlled nanoarchitecture.[2,10−13] Sensing units made by the LbL method for detection of different biocompounds have demonstrated a synergic effect between the biomolecules and the nanomaterial leading to highly sensitive and selective biosensors.[2,11,13] Especially for EIS structures, the first capacitive EIS sensor functionalized with an LbL film containing polyamidoamine (PAMAM) dendrimer and carbon nanotubes (CNT) was proposed with the enzyme penicillinase immobilized atop the film surface for detecting penicillin G. The use of this nanofilm as the host matrix for the penicillin immobilization generated a biosensor with high sensitivity toward penicillin G, also allowing for stable signals with low drift and fast response time.[14−18]

In this study, we demonstrate the efficiency of using LbL films made with dendrimer/carbon nanotubes as stabilizing matrixes for immobilization of the enzyme urease on capacitive EIS chips, followed by a study of the electrochemical properties for urea detection. This analyte is relevant in clinical diagnosis of renal and liver diseases, with its detection being performed

Received: January 24, 2014
Accepted: May 9, 2014
Published: May 9, 2014

   dx.doi.org/10.1021/ac500458s | *Anal. Chem.* 2014, 86, 5370−5375

frequently in medical care.[19−21] The signal stability of the urea-based EIS sensor and the influence of carbon nanotube incorporation in the film structure were investigated in three different arrangements: (1) atop of a bare EIS sensor, (2) atop of a 5-bilayer PAMAM/CNT nanofilm, and (3) embedded between a 5-bilayer PAMAM/CNT nanofilm and an additional CNT layer.

EXPERIMENTAL SECTION

Materials and Solutions. Carboxylic acid functionalized single-walled carbon nanotubes and fourth generation G4 PAMAM dendrimer were purchased from Sigma-Aldrich Co. CNTs were produced via the arc technique, with mainly semiconductor features, nominal purity of 95%, length of 0.5−1.5 μm, and diameter of 1.5−3.5 nm for individual and bundled samples. PAMAM and CNTs solutions were prepared at a concentration of 1.0 g L^{-1}, using titrisol buffer solution at pH 4 and pH 8, respectively. The CNT dispersion was obtained by adding 10 mg of the material into 10 mL of buffer solution under ultrasonication for 2 h and then filtrated three times.

Urease enzyme (*Canavalia ensiformis* made of Jack beans, 50 000−100 000 units/g solid) and urea were acquired from Sigma. The enzyme cocktail solution was prepared in phosphate buffer solution (PBS) at pH 7 by dissolving 60 mg of enzyme powder in 30 mL of buffer solution. Urea solutions were prepared at different concentrations ranging from 0.1 mM to 100 mM in a 0.25 mM polymix buffer solution at pH 8, containing 100 mM KCl solution as the ionic strength adjuster.

Fabrication of the EIS Sensors. The EIS structure consisted of a p-doped ⟨100⟩ silicon substrate (356−406 μm thick) with a specific resistance of ρ = 1−5 Ω cm. A 30 nm thick SiO_2 insulating layer was formed via a thermal oxidation under O_2 atmosphere at 1050 °C for 30 min. Afterward, a pH-sensitive Ta_2O_5 film with a thickness of ∼60 nm was deposited by electron-beam evaporation of 30 nm Ta, followed by thermal oxidation in an oxygen atmosphere at 520 °C for about 2 h. The validation of the layer thickness was carried out by using an ellipsometry Nanofilm EP^3 (Accurion, The Netherlands). A 300 nm thick aluminum film was electron-beam evaporated and deposited as a rear-side contact after removing the grown SiO_2 on the backside of the sensor with hydrofluoric acid. As a last step, the wafer was cut into single chips of 10 × 10 mm^2 sizes with a diamond saw. The EIS chips were mounted into a homemade measuring cell and sealed by an O-ring to protect the side walls and backside contact of the chip from solutions. The contact area of the EIS sensor with the solution was about 0.5 cm^2.

Fabrication of the PAMAM/CNT Nanofilms and Enzyme Immobilization. A homemade electrochemical acrylic cell, sealed with an O-ring, was used as a template to prepare the LbL films. The PAMAM/CNT nanofilm was assembled on EIS chips with the LbL technique, by alternately dropping 1 mL of the PAMAM (5 min) and 1 mL of the single-walled CNTs solution for 10 min each. This procedure was repeated five times to generate a film with five bilayers. We adopted the strategy of assembling five bilayers based on previous reports that demonstrate the formation of highly porous films with large surface area and without polymer packing.[16,17] Afterward, the film surface was rinsed with deionized water and dried under N_2 flow. The atop-film urease enzyme was obtained by dropping 200 μL of the enzyme cocktail onto the 5-bilayer PAMAM/CNT LbL nanofilm and dried under room temperature, being rinsed and stored in a 0.5 mM polymix buffer solution. For the sandwich configuration, 200 μL of the enzyme cocktail was dropped onto the 5-bilayer PAMAM/CNT LbL nanofilm followed by an additional CNT (500 μL) layer over the immobilized urease (adsorption time = 10 min). A schematic representation of the three urea-based biosensors investigated in this study is illustrated in Scheme 1.

Scheme 1. Schematic Representation of the Three Arrangements for the Urea-Based EIS Biosensors Investigated: (A) Urease Enzyme Atop of a Bare EIS Sensor, (B) Urease Enzyme Atop of a 5-Bilayer PAMAM/CNT LbL Film, and (C) Urease Enzyme between a 5-Bilayer PAMAM/CNT LbL Film and an Additional CNT Layer

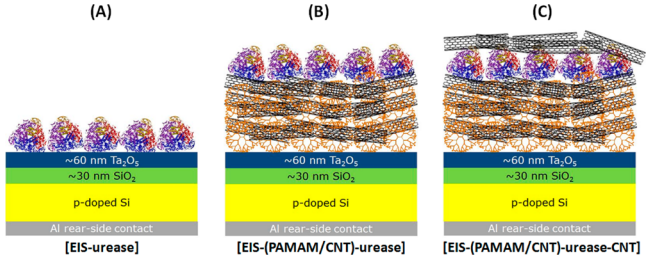

Measurement Setup. The surface morphology of the PAMAM/CNT LbL nanofilms and the adhesion of the urease enzyme layer on the film were analyzed by an atomic force microscope (AFM) BioMAT Workstation (JPK Instruments, Germany) in the tapping mode, using Si cantilevers with silicon nitride tips (8 nm radius). Images of the functionalized EIS sensors were taken in the constant height measuring mode at scanned areas of 1.0 × 1.0 μm^2 for all arrangements, and statistical quantities were analyzed by using the Gwyddion SPM data analysis. The urea biosensors were electrochemically characterized by means of impedance spectra (IS), capacitance−voltage (C/V) and constant-capacitance (ConCap) measurements using an impedance analyzer IM6 (Zahner Elektrik, Germany). The Bode IS was carried out in a frequency range varying from 1 Hz to 1 MHz at a polarization potential of 0 V vs Ag/AgCl for determination and evaluation of a specific low frequency in the capacitive region of the EIS-modified chips (see also Figure S1 in the Supporting Information). The C/V and ConCap characterizations were performed three times at a frequency of 30 Hz. During the operation, a conventional Ag/AgCl double-junction reference electrode (type 6.0726.100, Metrohm, Germany) with a salt bridge of 3 M KCl to set the working point of the EIS sensor was used. An ac voltage of 20 mV was also applied to the system in order to measure the capacitance. The contact area of the functionalized sensor surface was limited to 0.5 cm^2 by the reservoir of the measuring cell. All measurements were performed in a dark Faraday cage at room temperature.

RESULTS AND DISCUSSION

Surface Morphology of the Urea-Based EIS Sensor. The three arrangements of the urea-based EIS sensors were analyzed by AFM, with the results shown in Figure 1. Height-traced 3D AFM images revealed agglomerates (white spots) homogeneously distributed over the bare Ta_2O_5 surface (Figure 1A), which is ascribed to the immobilized urease enzyme, as demonstrated comparing this image with control images of a bare EIS chip without enzyme presence (see also Figure S2 in the Supporting Information). Figure 1B,C shows AFM images

dx.doi.org/10.1021/ac500458s | Anal. Chem. 2014, 86, 5370−5375

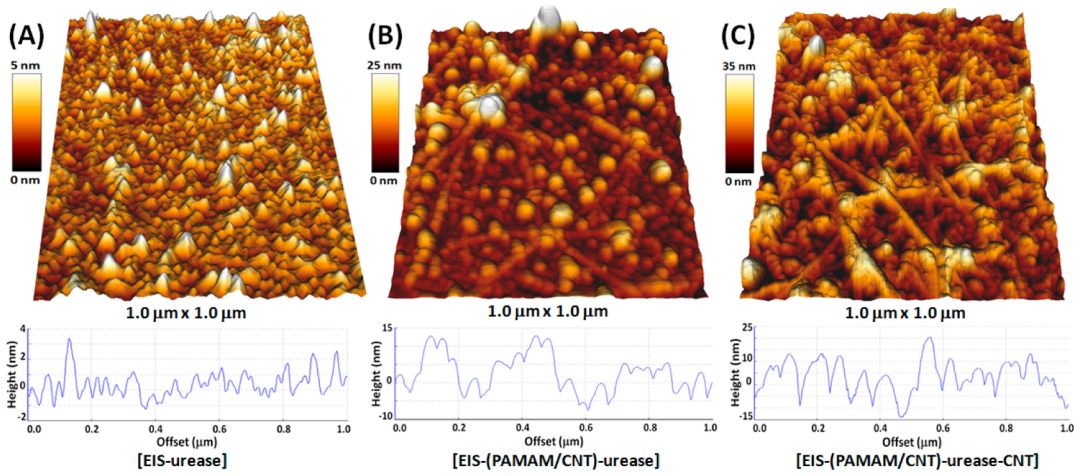

Figure 1. Height-traced 3D AFM images and line scans for the three urea-based EIS biosensor configurations: (A) urease enzyme atop of a bare EIS sensor, (B) urease enzyme atop of a 5-bilayer PAMAM/CNT LbL film, and (C) urease enzyme between a 5-bilayer PAMAM/CNT LbL film and an additional CNT layer.

of an enzyme layer atop of a 5-bilayer PAMAM/CNT nanofilm and sandwiched between the LbL film and an additional CNT layer, respectively. Figure 1B exhibited clearly the spherically shaped urease randomly and homogeneously covering the PAMAM/CNT film surface, while Figure 1C displays the presence of the additional CNT layer over the enzyme. Both images demonstrate the interpenetration of CNTs and enzyme molecules in a highly porous fashion with a large surface area. This latter is supported by line scans of each image that exhibits the increasing of the height profile among the three arrangements and is confirmed by the mean roughness (rms) of each sensor, as shown in Table 1. As expected, the sensor

Table 1. Mean Roughness (rms) Exhibited by the Three Urea-Based EIS Biosensor Arrangements

sensor configuration	rms roughness (nm)
EIS-urease	17.1
EIS-(PAMAM/CNT)-urease	18.8
EIS-(PAMAM/CNT)-urease-CNT	20.8

EIS-(PAMAM/CNT)-urease-CNT presented the higher height profile, leading to a higher roughness (rms) and larger surface area, demonstrating the influence of the nanofilm architecture on the morphological properties. The interconnection of nanotubes into the film can act as fast ionic-conducting channels, while the larger surface area permits a higher amount of enzyme immobilization and better distribution over the sensor surface. These features are desirable for sensor-based EIS structures, leading to enhanced sensing properties including stable signals and high sensitivity.

Note that the same amount of enzyme was immobilized for all three configurations. The arrangements containing the sensitive nanofilm (LbL-enzyme) were stable against several rinsing processes with aqueous solutions. On the other hand, the same did not occur for the bare EIS-enzyme arrangement, presenting a poor mechanical stability over the chip. This contrast confirms the suitability of using the PAMAM/CNT LbL film as host matrix for enzyme immobilization. Moreover, we have found in subsidiary experiments that other film-forming techniques, viz., casting or spin-coating, could not be used, as the resulting films were not as homogeneous and stable as for the LbL films.

Electrochemical Characterization and Urea Detection.

The biosensing ability toward urea of the modified EIS sensors was investigated by means of C/V measurements at urea concentrations ranging from 0.1 mM to 100 mM. Figure 2

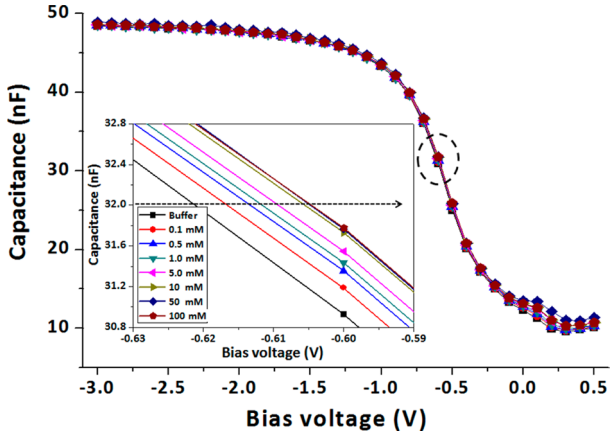

Figure 2. C/V curves at urea concentrations ranging from 0.1 mM to 100 mM for the arrangement with the enzyme atop the PAMAM/CNT LbL film. Inset: shift of the bias voltage to higher values with increasing urea concentrations at the sensor surface due to the enzymatic reaction.

presents results for the arrangement with the enzyme atop the PAMAM/CNT LbL film. The region between −1.0 and 0.0 V corresponds to the depletion zone that is intrinsic to the semiconductor EIS structure (p-Si−SiO_2−Ta_2O_5). Changes in this region indicate changes at the solid/liquid interface potential, thus modulating the flat-band voltage of the EIS sensor. In particular, the principle based on EIS sensors for urea detection consists of the enzymatic reaction,[19−21] as depicted in eq 1:

$$(NH_2)_2CO + 3H_2O \xrightarrow{\text{urease}} 2NH_4^+ + OH^- + HCO_3^- \quad (1)$$

The zoomed area around 32 nF in the inset shows the shift of the bias voltage to higher values with increasing urea concentrations, which indicates an increased OH^--ion concentration at the sensor surface due to the enzymatic reaction. It is

dx.doi.org/10.1021/ac500458s | Anal. Chem. 2014, 86, 5370−5375

stressed that the same behavior in the C/V curves was also observed for bare EIS-urease and EIS-(PAMAM/CNT)-urease-CNT sensors. The schematic illustration of the measurement setup and the operation principle of the urea biosensor-based EIS structure modified with a matrix film of PAMAM/CNT LbL film as well as the schematic representation of enzymatic reaction are depicted in Scheme 2.

Scheme 2. Scheme of the Measurement Setup Illustrating the Operation Principle and the Chemical Reaction for a Urea Biosensor-Based EIS Structure Modified with a Sensitive PAMAM/CNT LbL Nanofilm and the Enzyme Urease

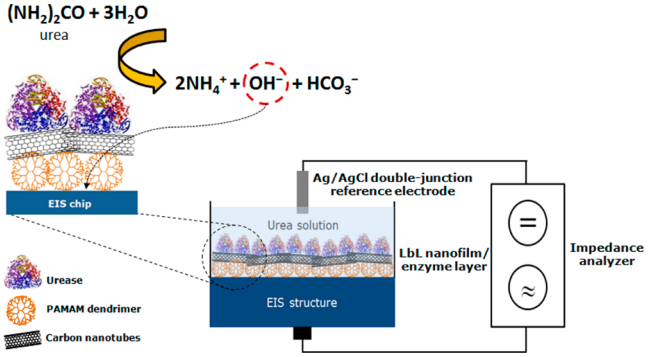

Furthermore, changes among the three sensors were observed in the maximum capacitance (C_{MAX}) behavior (see also Figure S3 in the Supporting Information). While the C_{MAX} values for the EIS-urease and EIS-(PAMAM/CNT)-urease sensors were recorded at approximately 48.0 nF and 47.0 nF, respectively, for the EIS-(PAMAM/CNT)-urease-CNT sensor a C_{MAX} value of around 44.0 nF was recorded. This implies that the overall capacitance of the EIS structure is decreasing with increasing layer thickness, which agrees with the theoretically expected behavior. The differences for each arrangement are related to the presence of additional layers on the EIS surface (LbL film, enzyme, and CNT). In terms of equivalent circuits, each arrangement corresponds to an additional parallel capacitor associated with the capacitive EIS structure.[7−9,22−24]

In order to investigate in detail the difference on the sensitive characteristics and to evaluate the biosensing ability of the modified urea-based EIS biosensors toward urea, ConCap measurements were further performed using the same range of urea concentrations (0.1 mM−100 mM). Figure 3 presents dynamic ConCap responses of urea concentrations for the bare EIS-urease (A), EIS-(PAMAM/CNT)-urease (B), and EIS-(PAMAM/CNT)-urease-CNT (C) sensor, respectively, as well as their corresponding calibration curves (D). The increase in OH^--ion concentration from the enzymatic reaction (owing to the catalyzed hydrolysis of urea into ammonium ions) in the presence of higher-concentrated urea solutions was determined from changes in the depletion potential at a fixed working point value of 32 nF. This capacitance value equals the flat-band region of the EIS field-effect sensor (see Figure 2). This region is typically selected in field-effect devices to study the influence of concentration changes of the analyte at the interface sensor/liquid, finally delivering a detectable electrochemical potential. All the sensors were sensitive for a low urea concentration of 0.1 mM. Considering the best linear range, viz., from 5 mM to 100 mM, both the bare EIS-urease and the EIS-(PAMAM/CNT)-urease sensors showed a similar signal response and sensitivity toward different urea concentrations. For these

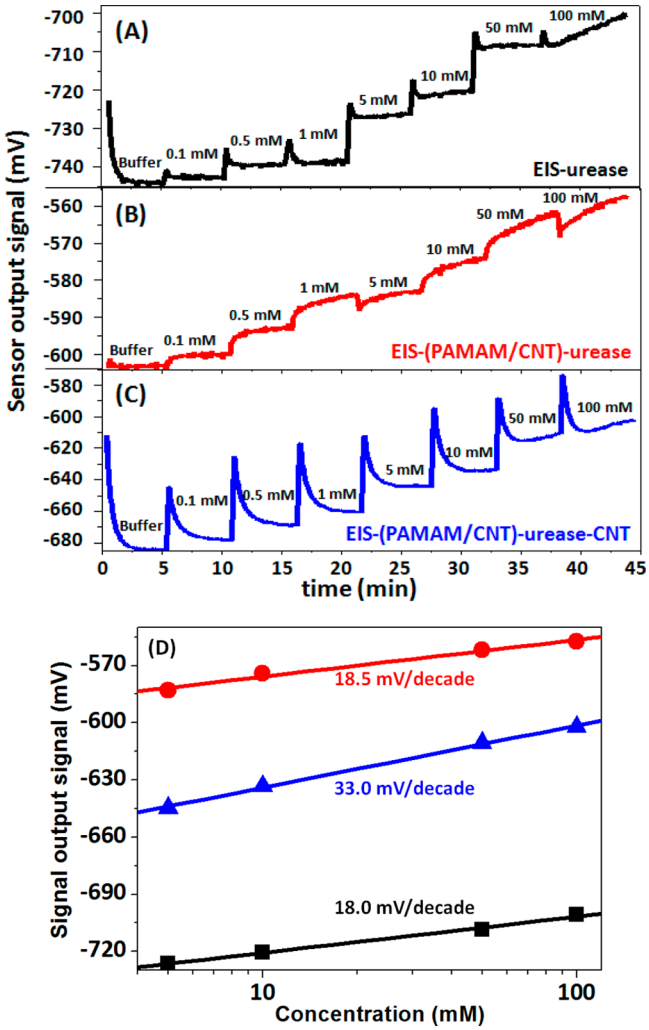

Figure 3. Dynamic ConCap responses for urea concentrations ranging from 0.1 mM to 100 mM for bare EIS-urease (A), EIS-(PAMAM/CNT)-urease (B) and EIS-(PAMAM/CNT)-urease-CNT (C) sensors, and their corresponding calibration curves (D).

sensors, the output signal increased somewhat irregularly after urea additions, exhibiting a sensitivity of 18 mV/decade (R = 0.996) and 18.5 mV/decade (R = 0.992) (Figure 3D) and a sensor drift of 0.2 mV/min and 1.1 mV/min, respectively.

In contrast, the EIS-(PAMAM/CNT)-urease-CNT sensor exhibited a linear output signal performance and higher sensitivity. Figure 3C shows clearly the constant increase of each potential step from lower to higher urea concentrations without saturation. Such enhancement in the detection signal led to a sensor with superior sensitivity toward urea of 33 mV/decade (R = 0.999). This value is almost 2-fold higher than for the other two sensor arrangements analyzed, as demonstrated in the calibration curve in Figure 3D. The stable detection signal, with a low drift of 0.5 mV/min, followed with the sensitivity achieved may envisage the application of this sensor arrangement to detect urea concentrations in human samples, like blood or urine.

For urea concentrations higher than 50 mM, the sensor signal enters into a drift regime and saturates for the three sensors configurations. This is a typical behavior for potentiometric enzyme sensors for higher-concentrated analytes. On the one hand, it indicates that the urea concentration is

dx.doi.org/10.1021/ac500458s | Anal. Chem. 2014, 86, 5370−5375

too high to be hydrolyzed completely by the urease enzyme, needing more time to stabilize the sensor output signal. On the other hand, at high urea concentrations, the pH change due to hydrolysis at the interface enzyme membrane/sensor surface is such strong that it additionally (negatively) influences the enzyme activity as well. These are two opposing effects. However, at 100 mM urea concentration, one may note a signal with lower drift for the EIS-(PAMAM/CNT)-urease-CNT sensor, leading to a faster stable response time. This might be attributed due to the fact that this sandwich-type, layered structure serves as a kind of diffusion barrier somewhat limiting the amount of substrate molecules at higher urea concentrations and, thus, extending the linear measurement range of the biosensor and demonstrating that the additional CNT layer incorporated atop the enzyme advantageously affects the electrochemical properties of the sensor.

A direct comparison with urea-based EIS sensors in the literature is difficult because diverse parameters such as the oxide layer employed as pH-sensitive ionic layer, supporting electrolyte, active area, and signal frequency are different. In addition, one has to consider the influence of membranes or nanofilms, which can modify the pH-sensitive behavior of the semiconductor transducer layer. Nevertheless, the performance of the EIS-(PAMAM/CNT)-urease-CNT, in terms of its output signal response, sensitivity, and detection limit, is superior or comparable to recent urea-based EIS biosensors, thus demonstrating the suitability of employing specific hybrid nanofilm-based nanotubes as stabilizer matrix for enzyme immobilization. For instance, Pan et al. introduced EIS devices employing diverse sensing membranes deposited on Si substrates by means of different physical deposition methods and applied them as urea biosensor. EIS devices with sensing membranes of Nd_2TiO_5 and TiO_2/Er_2O_3 as gate insulator membrane achieved a sensitivity around 9.0−10.0 mV/mM in a linear range of urea concentrations about 3−40 mM.[25,26] In another report, a urea-based EIS sensor with a sensing membrane of Sm_2O_3 exhibited a sensitivity of 2.45 mV/mM at a concentration range of 5−40 mM.[27] An EIS-based urea biosensor incorporating a PrY_xO_y sensing film presented a sensitivity of 9.59 mV/mM at a concentration range of 1−16 mM.[28] A sensitivity of 72.85 mV/p_{urea} at a concentration range of 0.1−32 mM was achieved for an EIS structure with a sensing layer of Sm_2TiO_5.[29] In the same concentration range, another report showed an EIS sensor with a novel high-k Dy_2TiO_5 sensing membrane with a sensitivity of 118.38 mV/pC.[30] In contrast to all these examples, the proposed $Al/Si/SiO_2/Ta_2O_5$ EIS structure has the advantage that the fabrication process is fully compatible with silicon planar technology that enables a cost-effective production with regards to future practical applications.[31]

Regarding electrochemical film stability, the arrangement LbL film-urease and LbL film-urease-CNT were stable on the EIS chip during the characterization period for urea detection. In contrast, a weak stability was observed with urease incorporated directly on the bare EIS surface, in which the enzyme layer starts to degrade after repeating the set of measurements for urea detection. Also worth mentioning was the selectivity toward urea of the sensor arrangements. In the course of experiments, highly concentrated glucose (50 mM) and polymix buffer solutions were alternately added with the urea solutions, but no signal changes were noted with either glucose or polymix buffer solutions. No signal response was also observed when bare EIS and EIS-(PAMAM/CNT) sensors, without enzyme immobilization, were submitted to urea detection. Once all the urea solutions were at the same adjusted pH value, no signal changes were observed.

The enhanced performance of the urea biosensor with the urease between the LbL film and the additional CNT layer may be explained based on a previous study, which correlates the morphological and chemical changes induced by the presence of carbon nanotubes on the sensitive film structure containing the enzyme urease.[32] It is already known that the combination dendrimer-nanotubes results in a host matrix nanofilm with a larger active surface area, which can allow both a better distribution and attachment of a higher amount of enzyme molecules immobilized on its surface.[15−17] The intimate contact between PAMAM and dense network bundles of CNTs form stable multilayers highly interconnected among them, resulting in a highly porous film. This porosity may offer easier ion penetration (in our case OH^--ions, see Scheme 2) from the enzymatic reaction onto the EIS surface. In the particular case, the additional nanotube layer when connected with the urease may lead to an enhancement of the enzyme activity due to fact that the enzyme becomes more stable into the film, causing a better molecular accommodation of the enzyme and facilitating the access of the catalytic substrate (urea). The assembled CNTs layer can interact with the LbL film and also with the enzyme layer in a noncovalent nature (van der Waals and electrostatic forces), permitting that CNTs interpenetrate into the urease layer and interact directly on the LbL film.[32] Therefore, the embedded nanotube layer atop the urease enzyme may act as a scaffold that stabilizes the enzyme molecules onto the EIS chip, preserving its catalytic sites, and thus enhancing the sensor performance with increasing sensitivity and signal response for urea detection.

■ CONCLUSIONS

In summary, we demonstrated that the use of the PAMAM/CNT LbL film as a matrix for urease immobilization with an additionally deposited nanotube layer atop the enzyme was decisive to achieve a urea-based EIS sensor with enhanced properties. In comparison to the EIS-urease and the EIS-(PAMAM/CNT)-urease sensors, the EIS-(PAMAM/CNT)-urease-CNT sensor exhibited an improved signal response and higher sensitivity assigned to the appropriate nanofilm structure, which created an adequate environment to allocate and to preserve the active sites of the enzyme urease on the sensor surface. An important implication of our findings is related to the possible use of this urea biosensor in real clinical assays, such as the determination of urine with high concentrations of interfering ions and lithogenic substances that usually can disturb the urea detection. Furthermore, to our knowledge, this is the first report on the utilization of such hybrid urease-carbon nanotube sensitive nanofilm for the detection of urea based on capacitive EIS sensors. We proved that the use of a PAMAM/CNT LbL film as host matrix for enzyme immobilization is entirely generic and may be extended to other enzymes, opening strategies for new capacitive EIS biosensors with superior and optimized performance.

■ ASSOCIATED CONTENT

Ⓢ Supporting Information

Additional information as noted in text. This material is available free of charge via the Internet at http://pubs.acs.org.

dx.doi.org/10.1021/ac500458s | Anal. Chem. 2014, 86, 5370−5375

AUTHOR INFORMATION

Corresponding Authors

*E-mail: jr.siqueira@fisica.uftm.edu.br. Phone: +55 34 3316 1818.

*E-mail: schoening@fh-aachen.de. Phone: +49 241 6009 53215.

Notes

The authors declare no competing financial interest.

ACKNOWLEDGMENTS

The authors are grateful to the Brazilian Foundations CNPq (Grant 480400/2010-5), FAPEMIG (Grant APQ-01064-12), and nBioNet network (CAPES) for the financial support. Furthermore, the authors gratefully thank Matthias Bäcker and Heiko Spelthahn for technical support.

REFERENCES

(1) Willner, I.; Willner, B. *Nano Lett.* **2010**, *10*, 3805−3815.

(2) Siqueira, J. R., Jr.; Caseli, L.; Crespilho, F. N.; Zucolotto, V.; Oliveira, O. N., Jr. *Biosens. Bioelectron.* **2010**, *25*, 1254−1263.

(3) Kim, S. N.; Rusling, J. F.; Papadimitrakopoulos, F. *Adv. Mater.* **2007**, *19*, 3214−3228.

(4) Allen, B. L.; Kichambare, P. D.; Star, A. *Adv. Mater.* **2007**, *19*, 1439−1451.

(5) Balasubramanian, K.; Burghard, M. *Anal. Bioanal. Chem.* **2006**, *385*, 452−468.

(6) Katz, E.; Willner, I. *ChemPhysChem* **2004**, *5*, 1085−1104.

(7) Schöning, M. J.; Poghossian, A. *Electroanalysis* **2006**, *18*, 1893−1900.

(8) Schöning, M. J. *Sensors* **2005**, *5*, 126−138.

(9) Schöning, M. J.; Poghossian, A. *Analyst* **2002**, *127*, 1137−1151.

(10) Ariga, K.; Ji, Q. M.; Mori, T.; Naito, M.; Yamauchi, Y.; Abe, H.; Hill, J. P. *Chem. Soc. Rev.* **2013**, *42*, 6322−6345.

(11) Iost, R. M.; Crespilho, F. N. *Biosens. Bioelectron.* **2012**, *31*, 1−10.

(12) Ariga, K.; Hill, J. P.; Lee, M. V.; Vinu, A.; Charvet, R.; Acharya, S. *Sci. Technol. Adv. Mater.* **2008**, *9*, 014109.

(13) Lutkenhaus, J. L.; Hammond, P. T. *Soft Mater.* **2007**, *3*, 804−816.

(14) Siqueira, J. R., Jr.; Abouzar, M. H.; Bäcker, M.; Zucolotto, V.; Poghossian, A.; Oliveira, O. N., Jr.; Schöning, M. J. *Phys. Status Solidi A* **2009**, *206*, 462−467.

(15) Siqueira, J. R., Jr.; Abouzar, M. H.; Poghossian, A.; Zucolotto, V.; Oliveira, O. N., Jr.; Schöning, M. J. *Biosens. Bioelectron.* **2009**, *25*, 497−501.

(16) Siqueira, J. R., Jr.; Werner, C. F.; Bäcker, M.; Poghossian, A.; Zucolotto, V.; Oliveira, O. N., Jr.; Schöning, M. J. *J. Phys. Chem. C* **2009**, *113*, 14765−14770.

(17) Siqueira, J. R., Jr.; Bäcker, M.; Poghossian, A.; Zucolotto, V.; Oliveira, O. N., Jr.; Schöning, M. J. *Phys. Status Solidi A* **2010**, *207*, 781−786.

(18) Siqueira, J. R., Jr.; Maki, R. M.; Paulovich, F. V.; Werner, C. F.; Poghossian, A.; de Oliveira, M. C. F.; Zucolotto, V.; Oliveira, O. N., Jr.; Schöning, M. J. *Anal. Chem.* **2010**, *82*, 61−65.

(19) Ruedas-Rama, M. J.; Hall, E. A. H. *Anal. Chem.* **2010**, *82*, 9043−9049.

(20) Duong, H. D.; Rhee, J. I. *Anal. Chim. Acta* **2008**, *626*, 53−61.

(21) Huang, C.-P; Li, Y.-K.; Chen, T.-M. *Biosens. Bioelectron.* **2007**, *22*, 1835−1838.

(22) Abouzar, M. H.; Poghossian, A.; Pedraza, A. M.; Gandhi, D.; Ingebrandt, S.; Moritz, W.; Schöning, M. J. *Biosens. Bioelectron.* **2011**, *26*, 3023−3028.

(23) Abouzar, M. H.; Siqueira, J. R., Jr.; Poghossian, A.; Oliveira, O. N., Jr.; Moritz, W.; Schöning, M. J. *Phys. Status Solidi A* **2010**, *207*, 884−890.

(24) Poghossian, A.; Abouzar, M. H.; Amberger, F.; Mayer, D.; Han, Y.; Ingebrandt, S.; Offenhäusser, A.; Schöning, M. J. *Biosens. Bioelectron.* **2007**, *22*, 2100−2107.

(25) Pan, T.-M.; Lin, J-.C.; Wu, M.-H.; Lai, C.-S. *Biosens. Bioelectron.* **2009**, *24*, 2864−2870.

(26) Pan, T.-M.; Lin, J-.C. *Sens. Actuators, B* **2009**, *138*, 474−479.

(27) Wu, M.-H.; Cheng, C.-H.; Lai, A.-S.; Pan, T.-M. *Sens. Actuators, B* **2009**, *138*, 221−227.

(28) Wu, M.-H.; Lee, C.-D.; Pan, T.-M. *Anal. Chim. Acta* **2009**, *651*, 36−41.

(29) Pan, T.-M.; Huang, M.-D.; Lin, W.-Y.; Wu, M.-H. *Anal. Chim. Acta* **2010**, *669*, 68−74.

(30) Pan, T.-M.; Lin, C.-W. *J. Electrochem. Soc.* **2011**, *158*, J100−J105.

(31) Schöning, M. J.; Brinkmann, D.; Rolka, D.; Demuth, C.; Poghossian, A. *Sens. Actuators, B* **2005**, *111−112*, 423−429.

(32) Caseli, L.; Siqueira, J. R., Jr. *Langmuir* **2012**, *28*, 5398−5403.